

Kerr Nonlinearity Dominance Diagnostic for Polarization-Dependent Loss Impaired Optical Transmissions

Matteo Lonardi⁽¹⁾, Paolo Serena⁽²⁾, Petros Ramantanis⁽¹⁾, Nicola Rossi⁽³⁾, Simone Musetti⁽⁴⁾

(1) Nokia Bell Labs, Paris-Saclay, France, matteo.lonardi@nokia-bell-labs.com

(2) Department of Engineering and Architecture, University of Parma, Parma, Italy

(3) Alcatel Submarine Networks, Paris-Saclay, France

(4) Nokia, Milan-Vimercate, Italy

Abstract We present a method to classify optical transmission systems as linear or nonlinear based solely on signal-to-noise ratio statistics in presence of PDL-induced time-varying-performance. It obtains excellent accuracy (>95%), and it is proven accurate and robust under all the investigated conditions.

Introduction

To keep up with the capacity increase, elastic optical networks (EON)^[1], in contrast to set-and-forget approach, represent a promising paradigm that focuses on transponders' operational flexibility to support self-management capability. One of EON's key enablers is the ability to accurately monitor linear and nonlinear effects to tailor configuration settings -including modulation format, symbol rate, spacing, and launch power- and enabling automation in tomorrow's networks.

Indeed, optical transmissions can be linear-dominated or nonlinear-dominated^{[2],[3]}, since a change in the optical launch power changes the impairment characteristics. At high power, the Kerr-induced nonlinear impairments (NLI) dominate. At low power, the Erbium doped-fiber amplifiers' (EDFA) amplified spontaneous emission (ASE) noise sets the transmission quality. Optical network architects may indulge one regime over the other for technical whys and wherefores; however, we usually aspire to work at the sweet spot of maximum performance: the nonlinear threshold (NLT)^[2], i.e., the optimal launch power maximizing the transmission quality and trading off linear ASE noise and NLI.

Consequently, researchers developed several machine-learning-based algorithms to detect the operational regime and quantify impairments by leveraging spectral or time-correlation properties of the received complex symbols or noise samples^{[4]-[8]}. The common trait

of these methods is to elaborate on received samples, which is a constraining factor if the computational transceiver resources are limited. Alternative solutions identify impairments based on the optical spectrum without the need to process receiver samples^{[9],[10]}. These solutions are potentially coherent-receiver-less and ubiquitous. Yet, they require spectrum analyzers along the line, resulting in an expensive option.

This paper introduces a computationally lightweight approach to discriminate between operational regimes (linear or nonlinear) based only on monitored performance and without introducing extra devices. The idea originates from observing two facts. First, terrestrial optical networks exhibit random performance oscillation due to polarization-dependent loss (PDL) introduced by network components, including EDFA and reconfigurable optical add-drop multiplexers (ROADM)^{[11],[12]}. Second, the PDL is shown to alter in different ways the random distributions of the received ASE noise and NLI^{[13],[14]}. Hence, monitoring the per-polarization signal-to-noise ratio (SNR) distribution provides enough information to diagnose the operating regime accurately.

The solution is designed to be deployed on the cheap in links that encounter PDL-induced fluctuating performance. Indeed, the increasing popularity of pluggable solutions in transparent terrestrial optical networks makes this approach a suitable candidate.

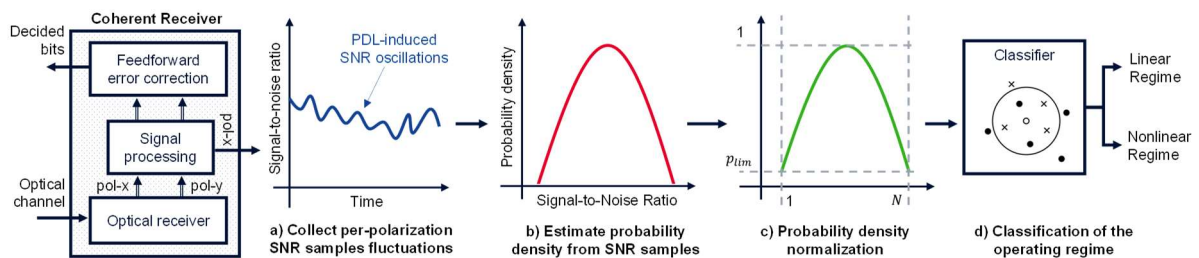


Fig. 1: The monitoring in brief. By observing the quality of transmission fluctuations, we derive statistical features to determine the operating regime, linear or nonlinear. After observing PDL-induced per-polarization SNR oscillations (a) we use their PDF distribution (b) after normalization (c) as a classifying feature (d).

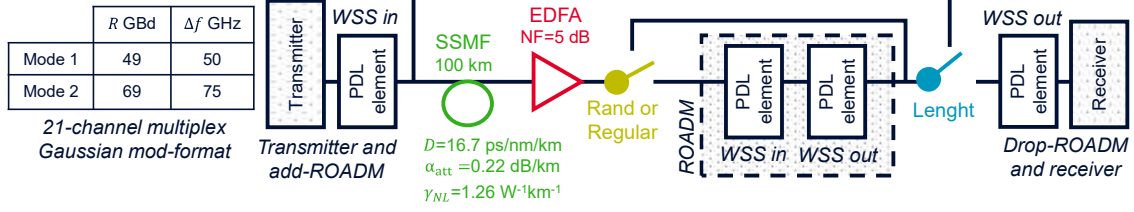


Fig. 2: Simulations setups. SSMF+EDFA spans repeat from transmitter to receiver. Depending on the setup pattern (regular or random) at each section a sequence of two PDL elements may emulate a ROADM (i.e., two WSS cascade). Every PDL element is tossed independently according to either chi-square (χ^2) or uniform (U) distributions.

Methodology

The method classifies optical transmissions as linear or nonlinear, i.e., operating below or above NLT. The steps in Fig. 1 lead to the classification. We observe that the PDL accumulated along the link (e.g., ROADMs, EDFAs) transforms the SNR of each polarization tributary in a random variable (Fig. 1.a), eventually generating a probability density function (PDF) (Fig. 1.b).

We collect SNR samples to obtain a PDF estimate, and then we proceed to normalization and data labeling. PDFs are framed in a specific rectangle, which specifies an SNR-level independent bin-grid and bounds the PDF values from 0 to 1 (Fig. 1.c). Pragmatically, from a PDF (Fig. 1.b), we cut tails at a given probability threshold, p_{lim} . The residual -central- part of the PDF is binned over a preset number of bins, N . This latter step removes SNR-level-related information. Then, every element is divided by the maximum value of the resulting vector. Eventually, we obtain an N -long vector with a maximum value of 1 (Fig. 1.c) which will be the input of the classifier. In our case $N=100$ and $p_{lim}=10^{-3}$. Further investigation can be done to find the optimal parameters, especially p_{lim} , which trades off classification performance and SNR collection time. Finally, every normalized vector is labeled with its class, “1” if linear ($P_{launch} < NLT$) or “0” if nonlinear ($P_{launch} \geq NLT$). After data labeling, we proceed to classification (Fig. 1.d), which is performed upon an initial training phase, i.e., supervised learning. We use

a k -nearest neighbors (k -NN, $k=10$) classifier.

Before moving to numerical results, we comment on the key benefits of the method. First, our approach is based on a minimal signal processing grounded on the per-polarization SNR, hence without the need of additional complex computations on the received symbols^{[4]–[8]}. Second, supervised learning-based monitoring is usually thorny to generalize to unseen scenarios. Indeed, training datasets must encompass all possible situations. However, we prove in this paper that the suggested method is highly adaptable to unseen scenarios and delivers excellent performance without the need to retrain. Indeed, by removing the SNR-level associated information, PDF shapes are not subject to substantial variations if transmission parameters, such as rate, spacing, or component’s PDL contributions, change^[15].

Simulations and Results

To validate the idea, we simulated many setups according to Fig. 2. Since the simulation of PDL in the nonlinear regime is particularly heavy, we used the Gaussian noise (GN) model extended to PDL, whose accuracy was validated in^[15]. In all scenarios, we use 21 Gaussian mod-format channels multiplex, targeting the central channel. We iteratively propagate over spans made by a standard single-mode fiber (SSMF) and an EDFA. After transmitter and before receiver, there is a ROADM in add or drop mode, i.e., a wavelength-selective switch (WSS) emulated by

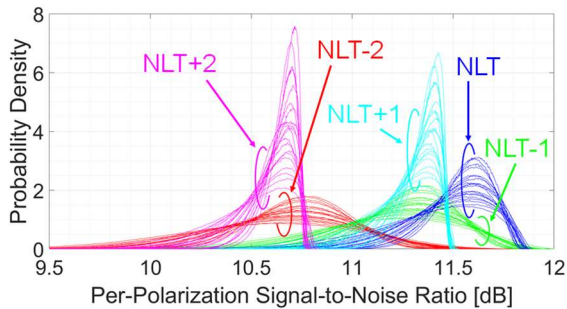


Fig. 3: SNR probability densities (Fig. 1.b) for 49 GBd and regular ROADM pattern at the 21st section (i.e., 21 fibers and 7 ROADMs). Every line represent a PDL-sequence realization and different colors are different powers, from $P_{launch}=NLT-2$ (linear) to $P_{launch}=NLT+2$ (nonlinear)

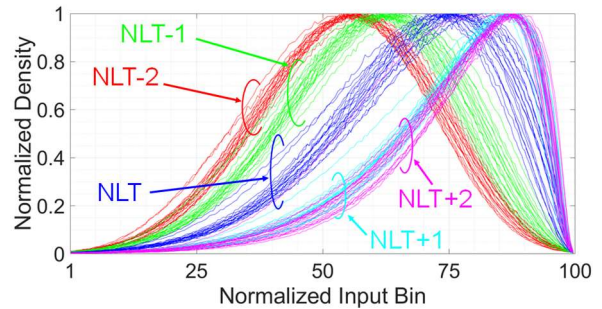


Fig. 4: Normalized vector at the classifier’s input (Fig. 1.c) for 49 GBd and regular ROADM pattern at the 21st section. Every line represent a PDL-sequence realization and different colors are different powers, from $P_{launch}=NLT-2$ (linear) to $P_{launch}=NLT+2$ (nonlinear).

Tab. 1: Accuracy Matrix

			Regular ROADM Pattern				Random Pattern		Test
			49 GBd		69 GBd		49 GBd	69 GBd	
Train			u	χ^2	u	χ^2	u	u	
Regular Pattern	49 GBd	u	-	97.0%	99.7%	97.6%	99.4%	99.2%	
		χ^2	99.1%	-	98.0%	99.5%	99.0%	98.8%	
	69 GBd	u	99.8%	96.2%	-	97.4%	99.4%	99.5%	
		χ^2	99.3%	99.2%	99.2%	-	99.3%	99.1%	
Ran. Pat.	49 GBd	u	99.0%	96.2%	99.3%	96.9%	-	99.6%	
	69 GBd	u	98.9%	95.6%	99.6%	96.6%	99.5%	-	

a PDL element without adding filtering penalties. For what concern transmission line, ROADM work in bypass mode, hence with two WSS. By varying transceiver and line setups we test six different scenarios which we describe in the reminder of this section. At the transceiver, we operate at 49 GBd with 50 GHz spacing (0.98 ratio) or at 69 GBd with 75 GHz spacing (0.92 ratio). Along the line, we test different number and positions of the ROADM and different PDL generation distributions. First, we have either a regular ROADM pattern, in which a ROADM cascades a series of 3 spans, or a random pattern, in which we randomly insert a ROADM at each span with 30% likelihood (Fig. 2 yellow switch). Second, we change the PDL-generation mechanism by tossing PDL values of each PDL element according to either uniform (u) distribution between 0.1 and 1 dB or chi-square (χ^2) distribution with 3 degrees of freedom (mean is 0.2130 dB and probability of exceeding 0.8 dB is 1.05%). For each PDL-generation mechanism, we investigate 20 random realizations of PDL elements. For every scenario, we investigate lightpath lengths of 12, 15, 18, and 21 spans (Fig. 2, blue switch), and swipe power from -10 to 10 dBm with 0.5 dBm steps. Finally, for data labeling, the optimal power, i.e., NLT, which separates linear and nonlinear regimes, is evaluated determining the power maximizing the SNR for each setup without PDL elements and swiping among all power levels. A total of about 20k simulations have been carried out.

Before moving to classification results, we detail an example of PDF and its normalization to explain the method's underlying idea. Fig. 3 shows PDFs (like Fig. 1.b) for 49 GBd and regular ROADM pattern at the 21st section for five different powers nearby NLT. Different colors are different powers, while different solid lines are transmissions corresponding to different PDL-generation seeds. Fig. 4 shows the normalized PDF (like Fig. 1.c) for the identical setup. We emphasize that SNR-level related information is removed passing from Fig. 3 to 4 and that PDFs are represented by 100-long vectors bounded in

0-1. Further, Fig. 4 reveals clustering for different powers independently of system configuration scrambling. We observe that in the linear regime, e.g., NLT-2 dBm, PDFs are almost symmetric. On the contrary, in the nonlinear regime, e.g., NLT+2 dBm, an asymmetry is clearly visible, induced by the interaction PDL-Kerr effects. A fast transitory between the two regimes emerges, which makes classification attractive.

To prove both accuracy and high adaptability of the method, we trained and tested with different scenarios, i.e., changing transmission and optical line parameters and, consequentially, changing the absolute value of the optimal launch power. Tab. 1 shows the results expressed by an accuracy matrix. Columns represent the testing scenario, while rows the training. On the diagonal, we have no values since it makes little meaning training and testing with the same dataset. At first, we see that we obtain excellent accuracy in every circumstance, with a minimum probability of correct classification of 95.6%. In general, we see that training with uniform and testing with chi-squared provides the lowest accuracy. However, the classification remains extremely reliable in all cases. Tab. 1 proves the good classification capabilities of the method and, at the same time, the possibility of learning and executing on different scenarios, i.e., the adaptability. Indeed, on top of presenting a computationally lightweight classifier, we deliver a highly versatile classification independent from the optical line and transceiver mode. The latter point might be helpful primarily to reach high-grade accuracy when data may be scarce^[16].

Conclusions

A new approach for regime classification (linear-nonlinear) in PDL-impaired optical transmissions is proposed. Unlike other methods, it elaborates on per-polarization SNR samples only, promising to be a low complexity solution. The method delivers accurate classification (>95%). It demonstrates excellent adaptability to a change of network conditions, which guarantees a robust solution even when real-field data is scarce.

References

- [1] P. Layec, A. Morea, F. Vacondio, O. Rival, and J. C. Antona, "Elastic optical networks: The global evolution to software configurable optical networks," *Bell Labs Tech. J.*, vol. 18, no. 3, pp. 133–151, 2013.
- [2] A. Bononi, N. Rossi, and P. Serena, "On the nonlinear threshold versus distance in long-haul highly-dispersive coherent systems," *Opt. Express*, vol. 20, no. 26, p. B204, 2012.
- [3] F. Vacondio *et al.*, "On nonlinear distortions of highly dispersive optical coherent systems," *Opt. Express*, vol. 20, no. 2, p. 1022, 2012.
- [4] A. S. Kashi *et al.*, "Fiber Nonlinear Noise-to-Signal Ratio Monitoring Using Artificial Neural Networks," in *European Conference on Optical Communication, ECOC*, 2017, vol. 2017-September, pp. 1–3.
- [5] F. J. Vaquero Caballero, D. Ives, Q. Zhuge, M. O'Sullivan, and S. J. Savory, "Joint estimation of linear and non-linear signal-to-noise ratio based on Neural Networks," in *Optical Fiber Conference (OFC)*, 2018.
- [6] F. J. Vaquero Caballero *et al.*, "Machine Learning Based Linear and Nonlinear Noise Estimation," *J. Opt. Commun. Netw.*, vol. 10, no. 10, pp. 42–51, 2018.
- [7] Z. Wang, A. Yang, P. Guo, and P. He, "OSNR and nonlinear noise power estimation for optical fiber communication systems using LSTM based deep learning technique," *Opt. Express*, vol. 26, no. 16, p. 21346, 2018.
- [8] Q. Zhuge *et al.*, "Application of Machine Learning in Fiber Nonlinearity Modeling and Monitoring for Elastic Optical Networks," *J. Light. Technol.*, vol. 37, no. 13, pp. 3055–3063, 2019.
- [9] M. Lonardi *et al.*, "Optical Nonlinearity Monitoring and Launch Power Optimization by Artificial Neural Networks," *J. Light. Technol.*, vol. 38, no. 9, pp. 2637–2645, 2020.
- [10] F. J. Vaquero Caballero *et al.*, "In-band perturbation based OSNR estimation," *arXiv*. 2020.
- [11] L. E. Nelson *et al.*, "Statistics of polarization dependent loss in an installed long-haul WDM system," *Opt. Express*, vol. 19, no. 7, p. 6790, 2011.
- [12] H. M. Chin *et al.*, "Probabilistic Design of Optical Transmission Systems," *J. Light. Technol.*, vol. 35, no. 4, pp. 931–940, 2017.
- [13] P. Serena *et al.*, "The Gaussian Noise Model Extended to Polarization Dependent Loss and its Application to Outage Probability Estimation," in *European Conference on Optical Communication, ECOC*, 2018, no. 1.
- [14] N. Rossi, S. Musetti, P. Ramantanis, and S. Almonacil, "The Impact of Kerr Nonlinearity on the SNR Variability Induced by Polarization-Dependent Loss," *J. Light. Technol.*, vol. 37, no. 19, pp. 5048–5055, 2019.
- [15] P. Serena, C. Lasagni, and A. Bononi, "The Enhanced Gaussian Noise Model Extended to Polarization-Dependent Loss," *J. Light. Technol.*, vol. 38, no. 20, pp. 5685–5694, 2020.
- [16] L. Torrey and J. Shavlik, "Transfer learning," in *Handbook of Research on Machine Learning*